

Will be submitted to *The Astrophysical Journal*

Follow-Up HST/STIS Spectroscopy of Three Candidate Tidal Disruption Events¹

S. Gezari, J. P. Halpern²

Department of Astronomy, Columbia University, 550 West 120th Street, New York, NY 10027-6601

suvi@astro.columbia.edu

S. Komossa

Max-Planck-Institut für extraterrestrische Physik, Giessenbachstrasse 1, D-85748 Garching, Germany

D. Grupe

Department of Astronomy, The Ohio State University, 140 West 18th Avenue, Columbus, OH 43210-1173

K. M. Leighly

Department of Physics and Astronomy, The University of Oklahoma, 440 W. Brooks St., Norman, OK 73019

ABSTRACT

Large amplitude, high luminosity soft X-ray flares were detected by the *ROSAT* All-Sky Survey in several galaxies with no evidence for Seyfert activity in their ground-based optical spectra. These flares had the properties predicted for a tidal disruption event by a central supermassive black hole: soft

¹Based on observations with the NASA/ESA Hubble Space Telescope obtained at the Space Telescope Science Institute, which is operated by the Association of Universities for Research in Astronomy, Incorporated, under NASA contract NAS5-26555. These observations are associated with proposal #9177.

²Visiting Astronomer, Kitt Peak National Observatory, National Optical Astronomy Observatories, which is operated by AURA, Inc., under a cooperative agreement with the National Science Foundation.

X-ray spectrum, time-scale of months, and large X-ray luminosity ($10^{42} - 10^{44}$ ergs s $^{-1}$). In order to evaluate the alternative hypothesis that these flares could have been some form of extreme AGN variability, we obtained follow-up optical spectroscopy of three of the flaring galaxies a decade later with the Space Telescope Imaging Spectrograph (STIS) and a narrow slit to search for or place stringent limits on the presence of any persistent Seyfert-like emission in their nuclei. Two of the galaxies, RX J1624.9+7554 and RX J1242.6–1119, show no evidence for emission lines or a non-stellar continuum in their *Hubble Space Telescope* (*HST*) nuclear spectra, consistent with their ground-based classification as inactive galaxies. They remain the most convincing as hosts of tidal disruption events. NGC 5905, previously known as a starburst H II galaxy due to its strong emission lines, has in its inner 0.1" a nucleus with narrow emission-line ratios requiring a Seyfert 2 classification. This weak Seyfert 2 nucleus in NGC 5905, which was masked by the many surrounding H II regions in ground-based spectra, requires a low level of prior non-stellar photoionization, thus raising some uncertainty about the nature of its X-ray flare, which may or may not have been a tidal disruption event. The absence of both broad emission lines and nuclear X-ray absorption in NGC 5905 also characterizes it as a “true” Seyfert 2 galaxy, yet one that has varied by more than a factor of 100 in X-rays.

Subject headings: galaxies: individual (NGC 5905, RX J1242.6–1119, RX J1624.9+7554) — galaxies: nuclei — galaxies: Seyfert — X-rays: galaxies

1. Introduction

Dormant, supermassive black holes, suspected to be present in the centers of many normal galaxies, should reveal themselves by a UV/X-ray flare when they tidally disrupt a star and some fraction of the tidal debris is accreted. Tidal disruption flares were proposed by Lidskii & Ozernoi (1979) and Rees (1988, 1990) as a probe for supermassive black holes in the centers of inactive galaxies. Such an event is very rare in the nucleus of a galaxy ($< 10^{-4}$ yr $^{-1}$); however, the *ROSAT* All-Sky Survey (RASS, Voges et al. 1999) conducted in 1990–1991 was an ideal experiment to detect these flares since it sampled hundreds of thousands of galaxies in the soft X-ray band. *ROSAT* detected soft X-ray outbursts from several galaxies with no previous evidence for Seyfert activity [see Komossa (2002) for a review]: NGC 5905 (Bade, Komossa, & Dahlem, 1996), RX J1242.6–1119 (Komossa & Greiner 1999), RX J1624.9+7554 (Grupe, Thomas, & Leighly, 1999), RX J1420+5334 (Greiner et al. 2000), and a possible fifth candidate, RX J1331–3243 (Reiprich & Greiner 2001). NGC 5905, RX

J1624.9+7554, and RX J1420+5334 were detected in the RASS, and then faded beneath the detection limits of the follow-up pointed observations, indicating variability by a factor > 100 on a time scale of months. RX J1242.6–1119 was serendipitously observed in the field of view of a pointed observation 18 months after its RASS non-detection, and was found to have increased in count-rate by a factor > 20 . In addition to the large amplitude of these flares, they were distinctive due to their extremely soft spectral indices ($2 \leq \Gamma \leq 5$) or blackbody temperatures ($kT_{\text{bb}} = 0.05 - 0.1$ keV), and high luminosities ($10^{42} - 10^{44}$ ergs s^{-1}). From the statistics of the RASS, Donley et al. (2002) calculated a rate of $\approx 1 \times 10^{-5}$ yr^{-1} for X-ray flares from these non-AGN galaxies.

Table 1 is a summary of the high-state *ROSAT* observations for the three galaxies studied in this paper, including the fitted power-law spectral index or blackbody temperature, corresponding 0.1–2.4 keV luminosities, absorbing column densities, estimated duration of the flare, and amplitude of variability. Previous authors ruled out various outburst scenarios due to their inconsistencies with the observed properties of the flares. Stellar sources such as X-ray binaries and supernovae rarely reach X-ray luminosities exceeding 10^{40} ergs s^{-1} . Gamma-ray burst afterglows could reach high enough peak luminosities, however, they have harder spectra and shorter durations than these flares, and are accompanied by bright optical afterglows. Gravitational lensing is another candidate for a high luminosity flare, but such an event would cause amplification at all wavelengths, not just in soft X-rays. The remaining outburst mechanisms that are able to produce the observed large flare luminosities require a central supermassive black hole. Soft X-ray variability due to varying obscuration or warm absorption of a Seyfert nucleus in NGC 5905 was examined in detail by Komossa & Bade (1999). Since no Seyfert-like narrow emission lines or broad Balmer lines were detected in ground-based optical spectra, their warm absorber model included dust to explain the absence of such optical emission. The dusty warm absorber did not allow an acceptable fit to the high-state and low-state *ROSAT* spectra without fine-tuning of the dust composition. With an obscured Seyfert nucleus as an unlikely fit, and no evidence for persistent Seyfert activity at any wavelength, an accretion disk instability was also disfavored as the cause for the soft X-ray outburst. A tidal disruption event by an otherwise quiescent central supermassive black hole arose as the most likely cause for the flares in these apparently inactive galaxies.

Throughout this paper, calculated and quoted luminosities are for $H_0 = 75 \text{ km s}^{-1} \text{ Mpc}^{-1}$ and $q_0 = 0.5$.

2. Theory of Tidal Disruption Events

When a star of mass m_* and radius R_* is in a radial “loss cone” orbit that brings it within the tidal radius of a central supermassive black hole, $R_T = (M_{\text{BH}}/m_*)^{1/3}R_*$, the tidal forces on the star are stronger than its self-gravity, and the star will be torn apart. For a solar type star, $R_T = R_{\odot}(M_{\text{BH}}/M_{\odot})^{1/3} = 1.1R_{\text{Sch}}M_8^{-2/3}$, where $M_8 = M_{\text{BH}}/10^8M_{\odot}$. If $M_{\text{BH}} > 1.1 \times 10^8M_{\odot}$, then the tidal radius is less than the Schwarzschild radius, and solar-type stars will not be disrupted, but will be swallowed whole by the black hole. For this mass range, red giants could be stripped of their outer layers, and solar-type stars could be disrupted if the black hole is spinning. The rate at which stars are disrupted by a central black hole depends on the mass of the black hole, the stellar density and velocities in the galactic nucleus, and the rate at which radial loss cone orbits are depleted. For typical nuclear stellar densities and velocities in the centers of galaxies, this results in a tidal disruption rate of $10^{-6}–10^{-4} \text{ yr}^{-1}$ (Magorrian & Tremaine 1999; Syer & Ulmer 1999). When a star is disrupted, half of the tidal debris will be ejected on hyperbolic orbits, half will return to pericenter and circularize, and a fraction of that bound debris will be accreted by the central black hole (Rees 1988). The return rate of this bound material on orbits that intersect at pericenter is what determines the time scales of the onset and decay of the luminosity resulting from a tidal disruption event. The observable flare would begin with accretion of the most tightly bound material as it returns to pericenter and circularizes. As summarized by Ulmer (1999), the first return would occur at a time t_0 after the disruption, where $t_0 \sim 1.1M_8^{1/2} \text{ yr}$. The maximum return rate, according to numerical simulations (Evans & Kochanek 1989) is $\dot{M}_{\text{max}} \sim 0.14M_8^{1/2}M_{\odot} \text{ yr}^{-1}$, and occurs at a time $t \sim 1.5t_0$. At late times, material returns at the declining rate $\dot{M}(t) = 0.3M_8(t/t_0)^{-5/3}M_{\odot} \text{ yr}^{-1}$, which is an important factor that controls the decay of the flare over the next few years. For $M_{\text{BH}} < 10^7M_{\odot}$, the dynamical time for the tidal debris is short relative to the return time, so the material is accreted quickly, resulting in a super-Eddington flare ($L_{\text{flare}} > \epsilon M_{\text{Edd}}c^2 > 1.3 \times 10^{46}M_8 \text{ ergs s}^{-1}$) (Ulmer 1999). For $M_{\text{BH}} > 2 \times 10^7M_{\odot}$, stellar debris takes a longer time to fall back than the rate at which it can circularize and radiate, thus accretion probably proceeds through a thin disk, with a luminosity always less than the Eddington limit. For a super-Eddington infall rate, the duration of the accretion flare is $t_{\text{flare}} \sim 0.76M_7^{-2/5} \text{ yr}$, and the spectrum of the flare will be characterized by the blackbody temperature of a thick disk or spherical envelope at the tidal radius, $T_{\text{eff}} \approx (L_{\text{Edd}}/4\pi\sigma R_T^2)^{1/4} = 3.0 \times 10^5M_7^{1/12} \text{ K}$ (Ulmer 1999). Thus, for low-mass central black holes ($M_{\text{BH}} < 10^7M_{\odot}$), tidal disruption theory predicts luminous flares of up to $10^{46} \text{ ergs s}^{-1}$, peaking in the UV/X-ray domain, with time scales on the order of months.

The three flaring galaxies studied in this paper had X-ray outbursts with properties predicted for a tidal disruption event: a high-state spectrum well-fitted by a soft blackbody

and a flare duration on the order of months. The galaxy with the best sampled X-ray light curve, NGC 5905, shows a fading of the flare luminosity close to the predicted accretion rate $\dot{M} \propto t^{-5/3}$ (Komossa & Bade 1999), which Li, Narayan, & Menou (2002) regard as strong evidence that its flare was a tidal disruption event. Although the tidal disruption hypothesis is appealing, there remains the possibility that low-luminosity Seyfert nuclei could reside in these galaxies, undetected in their low-states by ground-based optical observations. In order to establish beyond a reasonable doubt whether these flares were in fact tidal disruption events, as opposed to some other form of extreme AGN variability, we obtained follow-up *HST*/STIS spectroscopy through narrow slits, which are up to a factor of 100 more sensitive to nuclear activity than previously obtained ground-based spectra, to search for persistent Seyfert activity in the centers of these galaxies.

3. Observations and Basic Results

Long-slit spectra centered on the nuclei of RX J1242.6–1119A (the larger of a pair of galaxies at $z = 0.050$), RX J1624.9+7554 (a barred spiral at $z = 0.064$), and NGC 5905 (a large barred spiral at $z = 0.011$), were obtained a decade after their flares in Cycle 10 of *HST* with the STIS/CCD and either a $0.^{\prime\prime}2$ or a $0.^{\prime\prime}1$ slit. In each case, pairs of acquisition images were first obtained that were used to center the slit precisely on the nucleus of the galaxy. The STIS 2D spectra were reduced using the data calibration pipeline CALSTIS. After sky subtraction and bad-pixel removal, a 1D spectrum was rectified using a width in the spatial direction of $0.^{\prime\prime}36$, corresponding to 93.5% of the total energy in the point-spread-function (PSF). For comparison with the STIS spectra, ground-based spectra of comparable spectral resolution were obtained for each galaxy on the KPNO 2.1m and MDM 2.4m telescopes, with slits of width $1.^{\prime\prime}5 – 1.^{\prime\prime}9$. Table 2 is a log of STIS and ground-based observations. The STIS spectra of RX J1242.6–1119A and RX J1624.9+7554, shown in Figures 1 and 2, have stellar absorption features that are very similar to their ground-based optical spectra. Although the STIS spectra were obtained through a narrow slit, which explains the factor of $\sim 5 – 10$ weaker continuum levels compared to the ground-based spectra, there appears to be no difference in their spectral features or continuum shape. Some weak extended [N II] emission is seen in the KPNO 2.1m spectrum of RX J1624.9+7554, which was also detected in the ground-based spectrum of Grupe et al. (1999), and is most likely from the photoionized or shocked diffuse interstellar medium near the nucleus. Thus, there is no evidence for nuclear emission lines or a non-stellar continuum indicative of an AGN in RX J1242.6–1119A or RX J1624.9+7554. These two galaxies remain the most convincing as hosts of tidal disruption events, and will not be discussed further here. The remainder of this paper is concerned with evaluating the more problematic case of NGC 5905.

The STIS spectrum of NGC 5905, shown in Figures 3 and 4, contains Balmer and forbidden emission lines, including H α , H β , [O III], [O II], and [N II]. The ground-based spectra differ in both continuum level and relative narrow emission-line strengths. Most dramatic are the differences in the strength of [O III] $\lambda\lambda$ 4959,5007 relative to H β , and [N II] $\lambda\lambda$ 6548,6583 relative to H α . The forbidden lines are strongest relative to the Balmer lines in the STIS spectrum of the nucleus, whereas the STIS spectra offset to the east and west of the nucleus (Figure 4) have emission-line ratios similar to the ground-based spectrum. The blue-shifted H α and [N II] lines in the +1. $''$ 4 offset spectrum and the red-shifted lines in the -1. $''$ 2 offset spectrum align with the blue and red peaks of the double-peaked H α and [N II] lines in the STIS nuclear spectrum, which we interpret as rotation.

Figure 5 shows an H α rotation curve of the central 2 $''$ of NGC 5905 measured from the 2D STIS spectrum, in which the slit was oriented at position angle 99. $^{\circ}$ 4, nearly perpendicular to the bar. The red-shifted and blue-shifted components of the double-peaked nuclear H α line are seen to match the velocities of the outer rotation curve. This can be interpreted as a nuclear gas disk rotating in the same plane as the outer gas disk. The observed radial velocity semi-amplitude, $v_r = 114 \text{ km s}^{-1}$, is assumed to be the line-of-sight component of the circular rotation velocity v , where

$$v_r = \frac{v \cos i \sin i}{(\cos^2 i + \tan^2 \phi)^{1/2}} ,$$

i is the inclination angle of the rotation axis relative to the line of sight, and ϕ is the angle between the spectrograph slit and the major axis of the galaxy. Similarly, the projected distance d along the slit is related to the physical radius r in the galaxy via

$$d = r \cos i \left(\frac{1 + \tan^2 \phi}{\cos^2 i + \tan^2 \phi} \right)^{1/2} .$$

From the UGC catalog (Nilsson 1973) and other sources (van Moorsel 1982; Ma 2001), we adopt $i = 40^\circ$, and we determine that $\phi \approx 35.6^\circ$. For this set of parameters, we derive $v = 243 \text{ km s}^{-1}$, which is in excellent agreement with the maximum H I rotation velocity of 245 km s $^{-1}$ measured by van Moorsel (1982). Accordingly, the derived enclosed mass $M_{\text{enc}} = r v^2/G \leq 1.7 \times 10^8 M_\odot$ within an aperture $d < 11 \text{ pc} = 0.05''$ (half the width of the slit). This mass estimate is consistent with $M_{\text{BH}} \lesssim 1 \times 10^8 M_\odot$, and therefore in the appropriate mass range for causing the tidal disruption of a solar mass star.

Emission-line strengths in the STIS spectra of the nucleus of NGC5905 were measured using a wavelength interval of 27.4 Å for the low-resolution G430L spectrum, and 11.1 Å for the medium-resolution G750M spectrum (in order to include all the flux from the double-peaked profile of the lines). The neighboring continuum was estimated as the median value

in an interval of the same width on either side of the line, with the standard deviation in the continuum interval estimated as the 1σ error. The emission lines in the high signal-to-noise ground based-spectrum, shown in Figure 4, were measured using Gaussian fits to the lines. Table 3 lists the optical line fluxes relative to $\text{H}\alpha$ for both the STIS and ground-based spectra of NGC 5905. The nuclear spectrum is significantly reddened, as indicated by the ratio $\text{H}\alpha/\text{H}\beta = 11.8$. Also listed in Table 3 are the STIS line fluxes corrected for reddening using the extinction curve of Cardelli, Clayton, & Mathis (1989) and visual extinction $A_V = 4.26$ magnitudes, assuming intrinsic $\text{H}\alpha/\text{H}\beta = 3.1$ as is appropriate for Seyfert narrow-line regions (Halpern & Steiner 1983). This value of A_V should be considered an upper limit, as it does not take into account probable underestimation of the flux of $\text{H}\beta$ emission due to its superposition on stellar absorption from which it cannot be separated. When the double-peaked [N II] and $\text{H}\alpha$ lines in the STIS G750M nuclear spectrum are fitted with two Gaussians, the width of each Gaussian, corrected for instrumental resolution, is 130 km s^{-1} . The single-peaked [N II] and $\text{H}\alpha$ lines in the offset spectra are narrower, with an intrinsic width of 80 km s^{-1} . This difference indicates that there is a source of broadening in the nucleus in addition to rotation. The intrinsic width of the $\text{H}\beta$ and [O III] lines in the STIS G430L nuclear spectrum is 400 km s^{-1} , broader than the lines in the G750M nuclear spectrum, probably because the spectral resolution of the G430L spectrum is inadequate to resolve the double-peaked structure of the lines.

4. Interpretation

4.1. Ground-based Versus *HST* Post-flare Optical Spectra of NGC 5905

The post-flare ground-based and *HST* STIS spectra of NGC 5905 differ dramatically. The stellar continuum flux in the STIS spectrum is lower than the KPNO spectrum by two orders of magnitude, and the narrow emission line ratios in the STIS spectrum indicate a higher ionization state for the line emitting gas. The narrow emission line ratios measured from the KPNO spectrum identify NGC 5905 as a H II/starburst galaxy, consistent with the interpretation of previous ground-based spectra (Ho et al. 1997; Komossa & Bade 1999). The STIS spectrum of the nucleus of NGC 5905, on the other hand, has narrow emission-line ratios that place it in the Seyfert region of the diagnostic diagrams of Veilleux & Osterbrock (1987, see Figure 6). These differences in continuum flux and narrow emission-line ratios can be understood as a result of the narrower $0.^{\prime\prime}1$ slit used for the STIS spectrum as compared to the $1.^{\prime\prime}9$ slit of the KPNO spectrum, appropriate for ground-based seeing. The narrow slit effectively reduces the contribution of stellar light and circumnuclear H II region emission in the STIS spectrum, making it more sensitive to flux originating from the

nucleus itself. The narrow-line emission in the STIS spectrum is spatially compact compared to the stellar continuum (shown in Figure 7), indicating that the STIS has detected emission from a distinct source in the nucleus, namely, a low-luminosity Seyfert 2 nucleus that was previously masked by H II regions in the ground-based spectra.

4.2. Search for Non-Stellar Continuum & Broad Emission Lines

The post-flare STIS spectrum of NGC 5905 contains no broad Balmer line emission and no direct evidence for a non-stellar continuum. The Mg I b λ 5175 and G-Band λ 4300 stellar absorption features are detected in the STIS spectrum (shown with dotted lines in Figure 3), with equivalent widths consistent with the absorption features in the KPNO spectrum within 2σ , where $1\sigma \sim 1.2$ Å. The 1σ error includes the statistical error estimated from the neighboring continuum, and the systematic error from choosing the continuum level. The error in the equivalent widths places an upper limit on the percent contribution by a featureless continuum of 60%. This featureless continuum could be a power-law continuum from the Seyfert nucleus, or due to young stars. The Ca II H & K $\lambda\lambda$ 3968,3933 features and 4000 Å break are not obvious in the STIS spectrum, however their presence cannot be ruled out at this signal-to-noise level. It should be noted that the depth of the 4000 Å break is sensitive to the stellar population, as well as to the presence of an AGN continuum. The spatial profile of the acquisition image, shown in Figure 8, also does not indicate an AGN-like unresolved point source in the nucleus. Its radial profile is only slightly more concentrated than the confirmed inactive galaxies RX J1242.6–1119A and RX J1624.9+7554.

While these optical properties of NGC 5905 might be consistent with a Seyfert 2 nucleus having an obscured broad-line region and non-stellar continuum, the lack of X-ray absorption during the soft X-ray flare is a strong indicator that the direct line of sight to the nucleus is unobscured. Thus, the lack of broad emission lines is either intrinsic, or is evidence that the nucleus is in a quiescent state. The X-ray flare will have illuminated any gas around it with different light travel time delays. The observer will see reprocessed emission from an isodelay paraboloid, with the source of the flare at the focus. A point at a distance r from the flare and at angle θ from the line from the source to the observer will be illuminated with time delay $\tau = (1 - \cos \theta) r/c$. Gas in the line of sight ($\theta = 0^\circ$) will be illuminated with no time delay, and gas behind the nucleus ($\theta = 180^\circ$), will be observed to be illuminated with the maximum time delay of $2r/c$. Given that the STIS spectrum was obtained 11.4 years after the X-ray flare was observed, the smallest radial distance that the flare could be probing in the STIS spectrum is 1.7 pc, or 5.7 lyr. This is orders of magnitude larger than the scale of the broad-line region in Seyfert galaxies, which is typically on the order of light

days or weeks (e.g., Wandel, Peterson, & Malkan 1999). Therefore, we do not expect to see flare-excited broad-line emission in the STIS spectrum. In addition, since the high density typical of the broad-line region corresponds to rapid recombination times, fossil broad-line emission would not be expected either.

This result can be compared to observations of IC 3599, a *ROSAT* flaring galaxy that was observed optically only 5 months after its X-ray flare (Brandt, Pounds, & Fink 1995). In that case, strong Balmer emission lines and highly ionized [Fe VII] and [Fe X] lines characteristic of a Seyfert galaxy were detected. In the next spectrum obtained 9 months later, the highly ionized Fe lines had disappeared (Grupe et al. 1995). Henceforth, the optical spectrum of IC 3599 maintained the characteristics of a Seyfert galaxy (Grupe et al. 1995) of type 1.9 (Komossa & Bade 1999). Thus, the first post-flare spectrum had detected Fe emission from gas within 0.1 pc of the nucleus, ionized by the variable continuum. The opportunity to detect line emission from gas ionized by the flare very close to the nucleus in NGC 5905 was lost because the first post-flare optical spectrum was not obtained until 6 years after the event (Komossa & Bade 1999).

4.3. Narrow Emission Lines: Low-luminosity Seyfert 2 or Fossil Nebula?

Even in the absence of other evidence for Seyfert activity, the narrow emission-line ratios in the STIS spectrum of NGC 5905 require a non-stellar ionizing continuum. Two possibilities for the excitation of the line emission can be considered: narrow-line clouds ionized by a persistent, low-luminosity Seyfert nucleus, or the fossil nebula of the ionizing soft X-ray flare. If the emission lines are powered by a Seyfert nucleus, then the dereddened $H\alpha$ flux can be used to predict the time averaged soft X-ray luminosity of the nucleus using the correlation of soft X-ray luminosity with $H\alpha$ luminosity derived from observations of low-luminosity AGN ($L_X < 10^{42}$ ergs s^{-1}) by Halderson et al. (2001), who find $L_X = 7 L_{H\alpha}$ on average. The predicted soft X-ray luminosity of NGC 5905 is $\sim 4 \times 10^{40}$ ergs s^{-1} , consistent with the lowest value observed by the *ROSAT* PSPC ($L_X \approx 2 \times 10^{40}$ ergs s^{-1}), but the latter detection might also be partly associated with its nuclear starburst (Bade, Komossa, & Dahlem, 1996).

If the narrow emission lines are in fact powered by a Seyfert nucleus, then photoionization modeling can constrain the density and covering fraction f_c of the line-emitting gas. Using the photoionization code of Halpern & Steiner (1983), and similar works by Ferland (1981) and Ferland & Netzer (1983), we come to the following conclusions. The $H\beta$ luminosity as an indicator of the rate of absorption of ionizing photons yields $f_c Q(H) \approx 5.4 \times 10^{51}$ s^{-1} . Employing the ionization parameter $U = Q(H)/(4\pi r^2 n_H c)$, which must be $\sim 10^{-3}$ for the

excitation level indicated by the observed [O III]/H β flux ratio, we find $f_c n_H r^2 \approx 1.5 \times 10^{43} \text{ cm}^{-1}$. Since $r \leq 11 \text{ pc}$, we require $f_c n_H \geq 1.3 \times 10^4 \text{ cm}^{-3}$. The luminosity of the collisionally excited [O III] line also constrains the density and covering fraction of the line emitting gas. Assuming a plane-parallel geometry at a distance r from the nucleus, a thickness $\Delta r < r$ for [O III] zone of the cloud or filament, and a covering fraction f_c , the luminosity of [O III] is:

$$L(\text{[O III]}) = h\nu_{\text{[O III]}} 4\pi r^2 \Delta r n_{\text{O}^{++}} n_e q_{12} f_c \text{ ergs s}^{-1}$$

For a collisional excitation rate $q_{12} = 2.6 \times 10^{-9} \text{ cm}^3 \text{ s}^{-1}$ at $T = 15,000 \text{ K}$, $n_{\text{O}^{++}} = 10^{-4} n_e$, and a dereddened [O III] luminosity of $1.1 \times 10^{40} \text{ ergs s}^{-1}$, this implies an emission measure $r^2 \Delta r n_e^2 f_c = 8.5 \times 10^{62} \text{ cm}^{-3}$. Models indicate that $\Delta r n_e$ for the [O III] zone is $\approx 1 \times 10^{20} \text{ cm}^{-2}$ for $U \approx 10^{-3}$, so with $r \leq 11 \text{ pc}$ (half the width of the slit), we find $n_e f_c \geq 7300$. Another constraint on n_e comes from the [S II] density-sensitive line ratio, which indicates higher density in the nucleus than in the H II disk. Allowing for the large error bars on the fluxes of these weak lines, we find $0.3 < F(\lambda 6716)/F(\lambda 6731) < 1$ in the nucleus, which implies $n_e \geq 500$ (i.e., consistent with the high-density limit for this diagnostic). Thus, photoionized clouds of $n_H \sim 10^4$ and large covering fraction are consistent with the STIS spectrum of the nucleus. To the extent that we have overestimated the extinction, n_H and/or f_c might be smaller.

Although a persistent Seyfert nucleus cannot be ruled out as the source of the high excitation narrow emission lines, could the X-ray flare have produced these lines that we observe 11 years later? Using the blackbody fit to the *ROSAT* spectrum (which is more reasonable than a steep power-law, which would extrapolate to a bright optical flare that was not observed) the number of photons available to ionize hydrogen at the time of the flare can be estimated as those between the Lyman limit ν_0 and 100 eV,

$$Q(\text{H}) = \int_{\nu_0}^{100 \text{ eV}} \frac{L_\nu}{h\nu} d\nu = 4\pi R_{\text{bb}}^2 \frac{2\pi}{c^2} \left(\frac{kT}{h}\right)^3 \int \frac{x^2}{e^x - 1} dx = 1.5 \times 10^{51} \text{ photons s}^{-1},$$

where $R_{\text{bb}} = 9.2 \times 10^{10} \text{ cm}$ [corresponding to a 0.1 – 2.4 keV X-ray luminosity of $9.2 \times 10^{41} \text{ ergs s}^{-1}$ from Bade, Komossa & Dahlem (1996)] and $T = 6.5 \times 10^5 \text{ K}$. The predicted peak luminosities of H β $\lambda 4861$ and He II $\lambda 4686$ are

$$L = f_c h\nu \frac{\alpha_\nu^{\text{eff}}}{\alpha_B} \int_{\nu_0}^{100 \text{ eV}} \frac{L_\nu}{h\nu} d\nu \text{ ergs s}^{-1},$$

yielding $L = 5.4 \times 10^{38} f_c \text{ ergs s}^{-1}$ for H β and $1.6 \times 10^{39} f_c \text{ ergs s}^{-1}$ for He II, with $\nu_0(\text{He}) = 4\nu_0(\text{H})$. The dereddened STIS luminosity of H β is $1.9 \times 10^{39} \text{ ergs s}^{-1}$, 2.5 times greater than the peak luminosity powered by the flare, while He II is not detected with more than 2σ significance in the STIS spectrum, and can be assigned an upper limit of $6.5 \times 10^{38} \text{ ergs s}^{-1}$.

s^{-1} . The non-detection of the He II line in the STIS spectrum, which would be expected to be even stronger than the $\text{H}\beta$ line for gas ionized by the flare, is strong evidence that its emission lines are not powered by the flare, or if they are, that they must have decayed significantly.

The decay time for each emission line depends inversely on the density of the gas. Using the time-dependent photoionization model results of Binette & Robinson (1987), narrow-line emitting gas should continue to emit after the ionizing source (i.e., X-ray flare) has turned off. Although the [O III] line responds rapidly to the change in ionizing flux, and decays almost instantaneously due to efficient recombination by charge transfer, the He II and $\text{H}\beta$ lines will persist after the flare. Neglecting for the moment light travel time delays, the decay time for [O III] as a function of density is $\tau = 2000 n_{\text{H}}^{-1} \text{ yr}$, thus for $n_{\text{H}} > 180 \text{ cm}^{-3}$ the decay time is less than 11 years, and any [O III] emission excited by the flare will have decayed by now. The He II line has a decay time, $\tau = 23,500 n_{\text{e}}^{-1} \text{ yr}$, such that for $n_{\text{e}} < 2350 \text{ cm}^{-3}$, there should be fossil He II emission still detected in the post-flare spectrum 11 years later. Given the typical range of densities for narrow-line regions, if the line emitting gas were powered by a soft X-ray flare, the post-flare spectrum observed 11 years later should contain He II emission, but most if not all of the [O III] line emission will have decayed away. Given that [O III] is the stronger emission line compared to $\text{H}\beta$ and He II in the STIS spectrum, the narrow emission lines do not have flux ratios diagnostic of such a fossil nebula, i.e. $[\text{O III}]/\text{He II} \leq 1$ (Binette & Robinson 1987).

If we now allow for light travel time delays, we might hypothesize that the reason the narrow-line emission does not have line ratios characteristic of a fossil nebula is that we are seeing only clouds recently illuminated by the flare, and that differential rates of photoionization of various species could account for the strong [O III] emission relative to $\text{H}\beta$ and He II. The photoionization rate for hydrogenic ions is

$$\int_{\nu_0}^{100 \text{ eV}} \frac{F_{\nu}}{h\nu} \sigma_{\nu}(Z) d\nu \text{ s}^{-1}$$

where $F_{\nu} = L_{\nu}/4\pi r^2$ and $\sigma_{\nu}(Z)$ is the photoionization cross section as a function of atomic number Z . The resulting photoionization time scales at $r = 11 \text{ pc}$ (the half width of the STIS slit) are 115 days for H and 96 days for He. Similarly, the collisional excitation rate of [O III] at 15,000 K is $2.6 \times 10^{-9} \text{ cm}^3 \text{ s}^{-1}$, corresponding to a mean excitation time of $9(n_{\text{e}}/500)^{-1}$ days. Since the excitation times for all of these emission lines are very short relative to the light travel time between different parts of the narrow-line region, we would not expect to observe effects of photoionization delays.

If light-travel time delays are invoked to explain the continued presence of [O III] emission in the STIS post-flare spectrum of NGC 5905, then this argument cannot simultaneously

account for the absence of He II emission, which would be strong in recently ionized clouds. Thus, the line ratios in the STIS spectrum are not consistent with clouds photoionized by a soft X-ray flare, either near the nucleus and now decaying, or far from the nucleus and just being ionized. Therefore, the narrow line emission observed in NGC 5905 requires there to be a long-term source of ionization, i.e., a persistent Seyfert nucleus.

4.4. Geometry of the Line-Emitting Gas

If NGC 5905 in fact contains a Seyfert 2 nucleus, then according to the unified model it should be surrounded by a dusty torus that obscures emission in the line-of-sight from rapidly orbiting clouds in a broad-line region close to the central accreting black hole (Antonucci 1993). If this torus obscures the nucleus, then how could a soft X-ray flare have been observed from the vicinity of the black hole through such a high column density of X-ray absorbing gas? The column density derived from the *ROSAT* spectrum is close to the Galactic value, $1.5 \times 10^{20} \text{ cm}^{-2}$, while the Balmer decrement in the STIS spectrum corresponds to a column density of $8 \times 10^{21} \text{ cm}^{-2}$. This discrepancy might be addressed by invoking a higher than Galactic dust-to-gas ratio for the line emitting gas, or a gross error in the $\text{H}\alpha/\text{H}\beta$ measurement in the STIS spectrum due primarily to stellar absorption in those lines. However, neither effect is likely to be large enough to account for the factor of ≈ 50 difference in column density. A geometrical argument, on the other hand, could easily explain the observed optical extinction and lack of X-ray absorption if dusty line-emitting gas is distributed in a disk or torus in the plane of the galaxy and out of our line of sight to the nucleus. The double-peaked line profiles that match the rotation curve of the Galaxy also support this interpretation.

If the nucleus of NGC 5905 is not obscured by dust in the line-of-sight, then why does the STIS spectrum show only Seyfert 2 features? Halderson et al. (2001) found that Seyfert 2 galaxies in their sample of low-luminosity AGNs did not have systematically higher column density than Seyfert 1 galaxies in fits to *ROSAT* spectra. While this is contrary to the prediction of the unified model, they also attributed the apparent similarity in column density to the contamination by extended soft X-ray emission observed in both types of low-luminosity Seyfert galaxies. Ho et al. (2001) also found small column densities, $N_{\text{H}} < 10^{22} \text{ cm}^{-3}$, for most of the low-luminosity AGNs in their survey, including Seyfert 2s, suggesting that the unified model for Seyfert galaxies might not apply at low luminosities. An alternative interpretation of Seyfert 2 galaxies with small measured line-of-sight gas column densities is that they are “true” Seyfert 2s, with no broad line region, and any extinction is due to large-scale structures such as dust-lanes or circumnuclear starbursts. Panessa & Bassani (2002)

find that unobscured Seyfert 2's, with observed X-ray column densities $N_{\text{H}} < 10^{22} \text{ cm}^{-2}$, are biased towards lower luminosities. There is also mounting observational evidence that correlates a lower luminosity with a smaller broad line region (Wandel et al. 1999; Kaspi 2000; Collin & Huré 2001). This model can be extended to low enough luminosities that no broad line region exists (Tran 2001). An intrinsically weak Seyfert nucleus can also account for the non-detection of a featureless continuum in the STIS spectrum, and the lack of optical variability (within ~ 0.2 mag) during the flare as reported by Komossa & Bade (1999) from photographic plates. Thus, NGC 5905 may have an intrinsically weak non-stellar continuum, no broad line region, and only narrow-line clouds available to be ionized. A final possibility to consider is that the *HST*/STIS observations could have occurred during a low-state of the Seyfert nucleus, when the ionizing continuum and broad line region emission are temporarily “off”.

5. Conclusions

RX J1242.6–1119A and RXJ1624.9+7554 are confirmed to be inactive galaxies from the lack of broad or narrow emission lines, or a non-stellar continuum in their narrow-slit *HST*/STIS spectra. The most likely explanation for large amplitude X-ray flares from the nuclei of inactive galaxies is a tidal disruption of a star by an otherwise dormant central supermassive black hole.

An important question is raised in the case of NGC 5905: whether its X-ray flare was the result of large amplitude variability of its low-luminosity Seyfert nucleus, or a tidal disruption event. Both scenarios involve a dramatic increase in the rate of accretion onto the central black hole, either by an instability in a preexisting accretion disk, or by the formation of a debris disk from the tidally disrupted star. We use emission-line diagnostics to show that a persistent Seyfert nucleus in NCG 5905 is required to account for its nuclear emission lines, which we resolved from the surrounding H II regions using *HST*/STIS spectroscopy. While not ruling out the possibility that the soft X-ray flare was a tidal disruption event, this prior activity does raise some uncertainty about such an interpretation. The nuclear emission-line luminosities correspond to an average X-ray luminosity of $\approx 4 \times 10^{40} \text{ ergs s}^{-1}$, which is similar to the lowest value seen by *ROSAT* after the flare. Further long-term monitoring in the X-ray and optical is necessary to see whether flaring behavior in NGC 5905 recurs, which would indicate variability intrinsic to the Seyfert nucleus, or whether its X-ray flare was a one-time event consistent with the expected frequency of tidal disruption. If the flare was not a tidal disruption event, it is one of the most extreme cases of X-ray variability observed sofar among AGN. A separation of nuclear and starburst X-ray sources in NGC 5905 can be

accomplished by *Chandra*, which could then establish the minimum X-ray luminosity of the nucleus by repeated observations.

It is important to find unambiguous indicators of tidal disruption events. If they have properties similar to the candidates studied here, then future UV and X-ray sky surveys will have the potential to detect hundreds of tidal disruption events, making it possible to study the masses of black holes as a function of galaxy type and size, unbiased by the minority of galaxies that are AGNs, and to a much larger distance than those that can be studied using stellar dynamics.

We thank Mike Eracleous for his help with observations and reduction of ground-based spectra. Support for Proposal #9177 was provided by NASA through a grant from the Space Telescope Science Institute, which is operated by the Association of Universities for Research in Astronomy, Incorporated, under NASA contract NAS5-26555.

REFERENCES

Antonucci, R. 1993, *ARA&A*, 31, 473

Bade, N., Komossa, S., & Dahlem, M. 1996, *A&A*, 309, L35

Binette, L., & Robinson, A. 1987, *A&A*, 177, 11

Brandt, W. N., Pounds, K. A., & Fink, H. 1995, *MNRAS*, 273, L47

Cardelli, J. A., Clayton, G. C., & Mathis, J. S. 1989, *ApJ*, 345, 245

Collin, S., & Huré, J.-M. 2001, *A&A*, 372, 50

Donley, J. L., Brandt, W. N., Eracleous, M., & Boller, Th. 2002, *AJ*, 124, 1308

Ferland, G. 1981, *ApJ*, 249, 17

Ferland, G., & Netzer, H. 1983, *ApJ*, 264, 105

Greiner, J., Schwarz, R., Zharikov, S., & Orio, M. 2000, *A&A*, 362, L25

Grupe, D., Beuermann, K., Mannheim, K., Bade, N., Thomas, H.-C., de Martino, D., & Schwone, A. 1995, *A&A*, 229, L5

Grupe, D., Thomas, H. C., & Leighly, K. M. 1999, *A&A*, 350, L31

Halpern, J. P., & Steiner, J. E. 1983, ApJ, 269, L37

Halderson, E.L., Moran, E. C., & Filippenko, A. V. 2001, ApJ, 122, 637

Ho, L.C., Filippenko, A. V., & Sargent, W. L. W. 1997, ApJ, 487, 568

Kaspi, S., Smith, P. S., Netzer, H., Maoz, D., Jannuzi, B. T., & Giveon, U. 2000, ApJ, 533, 631

Komossa, S. 2002, in Lighthouses of the Universe, (ESO: Garching), 463

Komossa, S., & Bade, N. 1999, A&A, 343, 775

Komossa, S., & Greiner, J. 1999, A&A, 349, L45

Li, L.-X., Narayan, R., & Menou, K. 2002, ApJ, 576, 753

Lidskii, V. V., & Ozernoi, L. M. 1979, PAZh, 5, L28

Ma, J. 2001, Chinese J. Astron. Astrophys., 1, 395

Magorrian, J., & Tremaine, S. 1999, MNRAS, 309, 447

Nilson, P. 1973, The Uppsala General Catalogue of Galaxies (Uppsala: Uppsala Astron. Obs.)

Panessa, F., & Bassani, L. 2002, A&A, 394, 435

Rees, M. 1988, Nature, 333, 523

Rees, M. 1990, Science, 247, 817

Reiprich, T. H., & Greiner, J. 1999, in Black Holes in Binaries and Galactic Nuclei, eds L. Kaper, E. P. J. van den Heuvel, & P. A. Woudt (Springer), 168

Syer, D., & Ulmer, A. 1999, MNRAS, 306, 35

Tran, H. D. 2001, ApJ, 554, L19

Ulmer, A. 1999, ApJ, 514, 180

van Moorsel, G. A. 1982, A&A, 107, 66

Veilleux, S., & Osterbrock, D. E. 1987, ApJS, 63, 295

Voges, W. et al. 1999, A&A, 349, 389

Wandel, A., Peterson, B. M., & Malkan, M. A. 1999, ApJ, 526, 579

This preprint was prepared with the AAS L^AT_EX macros v5.0.

Table 1. Summary of *ROSAT* Observations

Galaxy	Date	Γ ($N(E) \propto E^{-\Gamma}$)	L_X (pl) (ergs s ⁻¹)	kT _{bb} (eV)	L_X (bb) (ergs s ⁻¹)	N_H (Gal) (cm ⁻²)	t _{flare} (months)	Variability Amplitude
RXJ1242.6–1119A	1992 Jul	5.1 ± 0.9	1.42×10^{44}	60 ± 1	3.5×10^{43}	3.74×10^{20}	< 18	> 20
RXJ1624.9+7554	1990 Oct	2.29 ± 0.12	1.1×10^{44}	97 ± 4	1×10^{44}	3.9×10^{20}	< 18	> 200
NGC 5905	1990 Jul	4.0 ± 0.4	6.1×10^{41}	56 ± 12	9.2×10^{41}	1.5×10^{20}	~ 5	> 120

Table 2. Log of Post-Flare Optical Spectra

Galaxy	Date	Telescope	Grating or Spectrograph	Slit Width (arcsec)	Wavelength Range (Å)	Resolution (Å)	t_{exp} (min)
RXJ1242.6–1119A	2001 Aug 9	<i>HST</i> /STIS	G430L	0.2	2900–5700	4.1	91.5
	2001 Aug 9	<i>HST</i> /STIS	G750L	0.2	5240–10270	7.9	79.8
	2000 Jun 4	KPNO 2.1m	Goldcam	1.9	3900–7500	5	30.0
	2000 Jun 1	MDM 2.4m	CCDS	1.5	3200–6800	12	30.0
RXJ1624.9+7554	2001 Oct 1	<i>HST</i> /STIS	G430L	0.2	2900–5700	4.1	101.5
	2001 Oct 1	<i>HST</i> /STIS	G750L	0.2	5240–10270	7.9	92.2
	2000 Jun 4	KPNO 2.1m	Goldcam	1.9	3900–7500	5	30.0
	1999 Feb 9	MDM 2.4m	MkIII	1.7	4000–8600	5	40.0
NGC 5905	2001 Dec 20	<i>HST</i> /STIS	G430L	0.1	2900–5700	3.8	37.2
	2001 Dec 20	<i>HST</i> /STIS	G750M	0.1	6295–6867	0.8	49.7
	2000 Jun 4	KPNO 2.1m	Goldcam	1.9	3900–7500	5	15.0
	2000 Jun 1	MDM 2.4m	CCDS	1.5	3200–6800	12	15.0

Table 3. NGC 5905 Post-flare Optical Line Fluxes

Line	KPNO 2.1m	<i>HST</i> /STIS	Dereddened
[O II] λ 3727	...	0.19 ± 0.01	3.20 ± 0.24
He II λ 4686	< 0.03	< 0.02	< 0.11
H β λ 4861	0.27	0.08 ± 0.01	0.32 ± 0.03
[O III] λ 4959	0.05	0.22 ± 0.02	0.75 ± 0.06
[O III] λ 5007	0.12	0.58 ± 0.03	1.88 ± 0.09
[O I] λ 6300	< 0.03	0.16 ± 0.04	0.19 ± 0.05
[N II] λ 6548	0.15	0.53 ± 0.05	0.53 ± 0.05
H α λ 6563	1.00 ^a	1.00 ± 0.06^b	1.00 ± 0.06^c
[N II] λ 6583	0.44	1.53 ± 0.07	1.51 ± 0.07
[SII] λ 6716	0.14	0.11 ± 0.04	0.10 ± 0.04
[SII] λ 6731	0.11	0.18 ± 0.03	0.16 ± 0.03

^aF(H α) = 3.7×10^{-14} ergs cm $^{-2}$ s $^{-1}$.

^bF(H α) = 1.0×10^{-15} ergs cm $^{-2}$ s $^{-1}$.

^cF(H α) = 2.4×10^{-14} ergs cm $^{-2}$ s $^{-1}$.

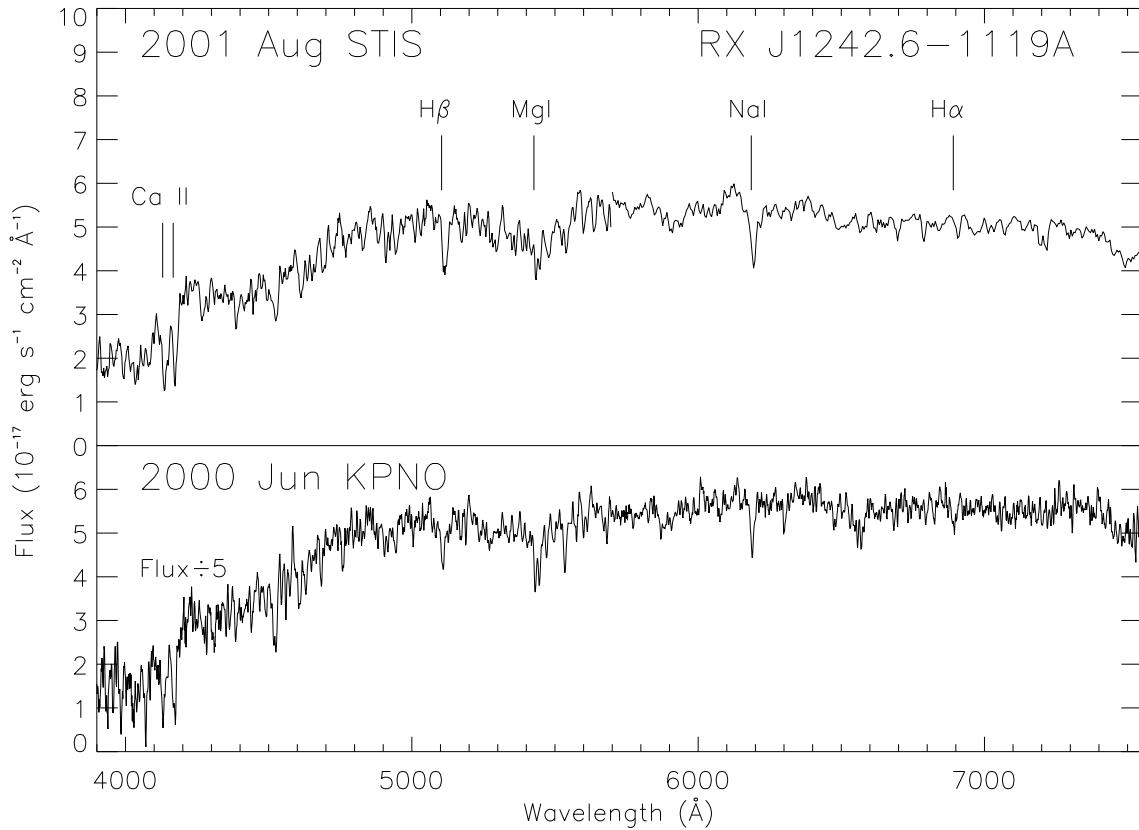


Fig. 1.— Post-flare spectra of RX J1242.6–1119A from *HST*/STIS and the KPNO 2.1m, smoothed over one spectral resolution element. The KPNO spectrum has been divided by a factor of 5 for comparison. Both spectra show only stellar absorption features, with no evidence of high excitation emission lines or a non-stellar continuum indicative of an AGN.

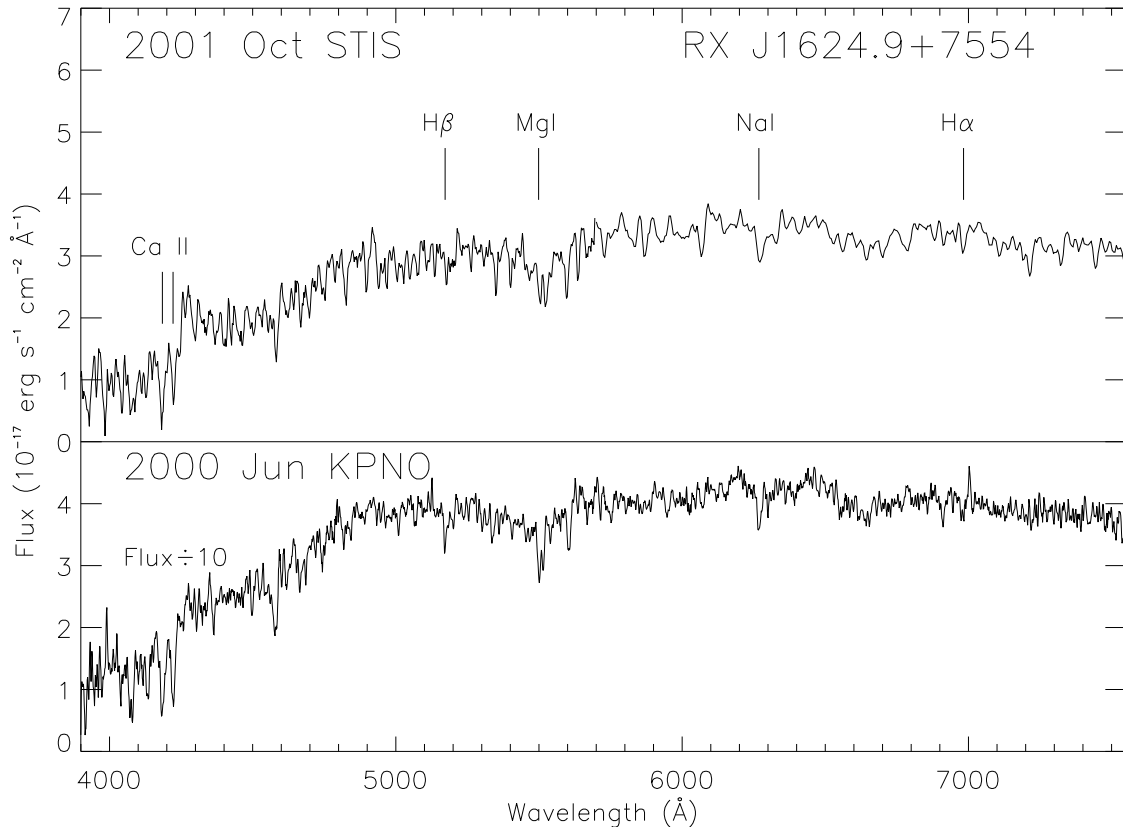


Fig. 2.— Post-flare spectra of RX J1624.9+7554 from *HST*/STIS and the KPNO 2.1m, smoothed over one spectral resolution element. The KPNO spectrum has been divided by a factor of 10 for comparison. Both spectra show similar stellar absorption features, with no evidence of high-excitation emission lines or a non-stellar continuum indicative of an AGN. Weak, extended [N II] λ 6583 emission is detected in the KPNO spectrum, most likely associated with H II regions near the nucleus.

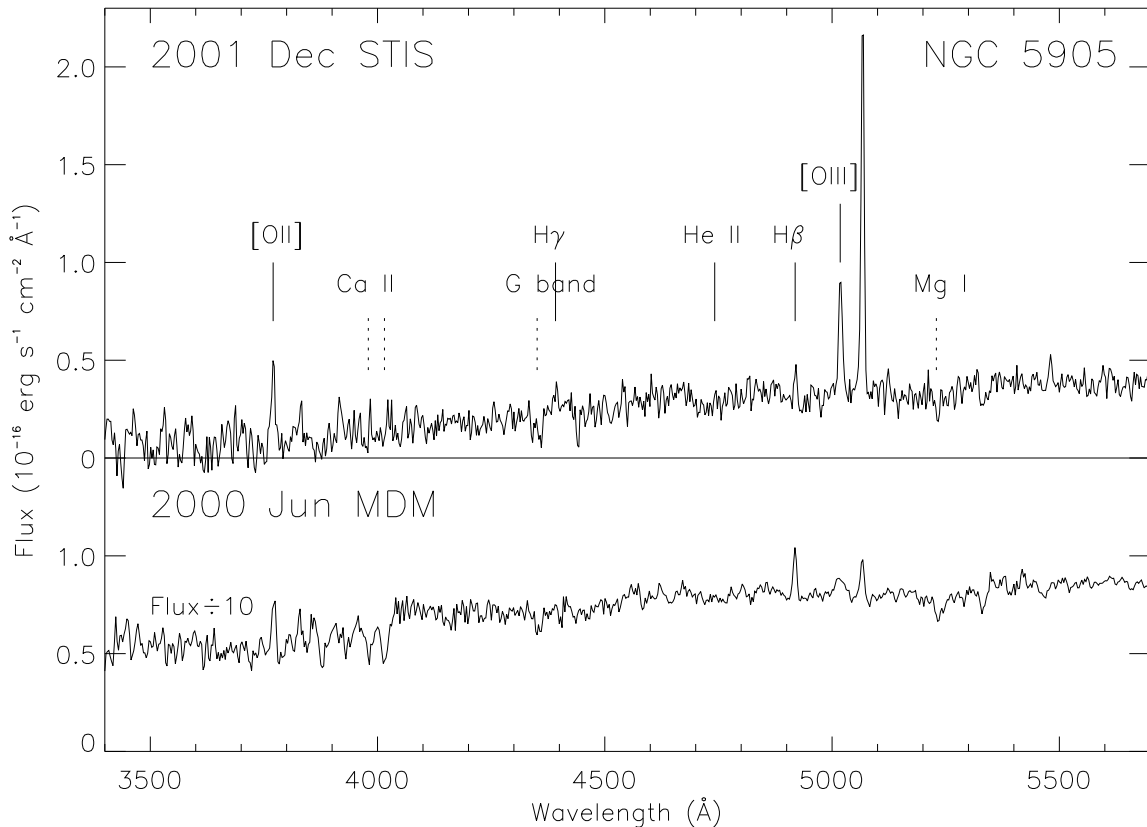


Fig. 3.— Post-flare spectra of the nucleus of NGC 5905 from *HST*/STIS and the MDM 2.4m, smoothed over one spectral resolution element. The MDM spectrum has been divided by 10 for comparison. The STIS spectrum has narrow-line emission consistent with a Seyfert 2 nucleus, in contrast to the MDM spectrum which is classified as an H II/starburst. Stellar absorption features, shown with dotted lines, are observed in both the STIS and ground-based nuclear spectra, indicating the lack of a strong non-stellar continuum.

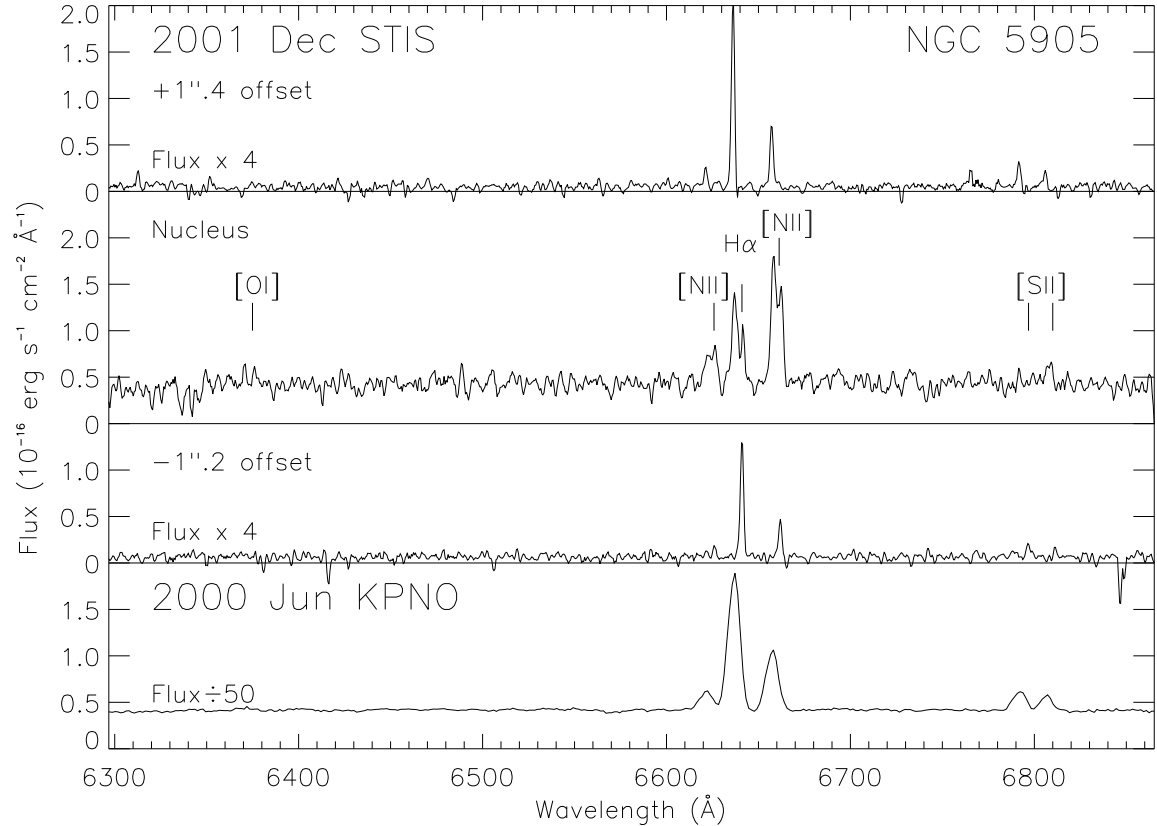


Fig. 4.— Post-flare *HST*/STIS spectra of the nucleus of NGC 5905 with the G750M grating, as well as regions of peak H II emission offset $+1''.4$ and $-1''.2$ from the nucleus, smoothed over one spectral resolution element. The off-nuclear STIS spectra have been multiplied by 4 for comparison. A spectrum from the KPNO 2.1m, divided by 50, is shown for comparison. The STIS spectrum has narrow-line emission consistent with a Seyfert 2 nucleus, while the off-nuclear STIS spectra and ground-based spectrum have narrow-line emission consistent with an H II/starburst. The double peaks of H α and [N II] emission in the nuclear STIS spectrum match the velocity shifts of the off-nuclear spectra, which can be ascribed to the rotation curve (see Figure 5).

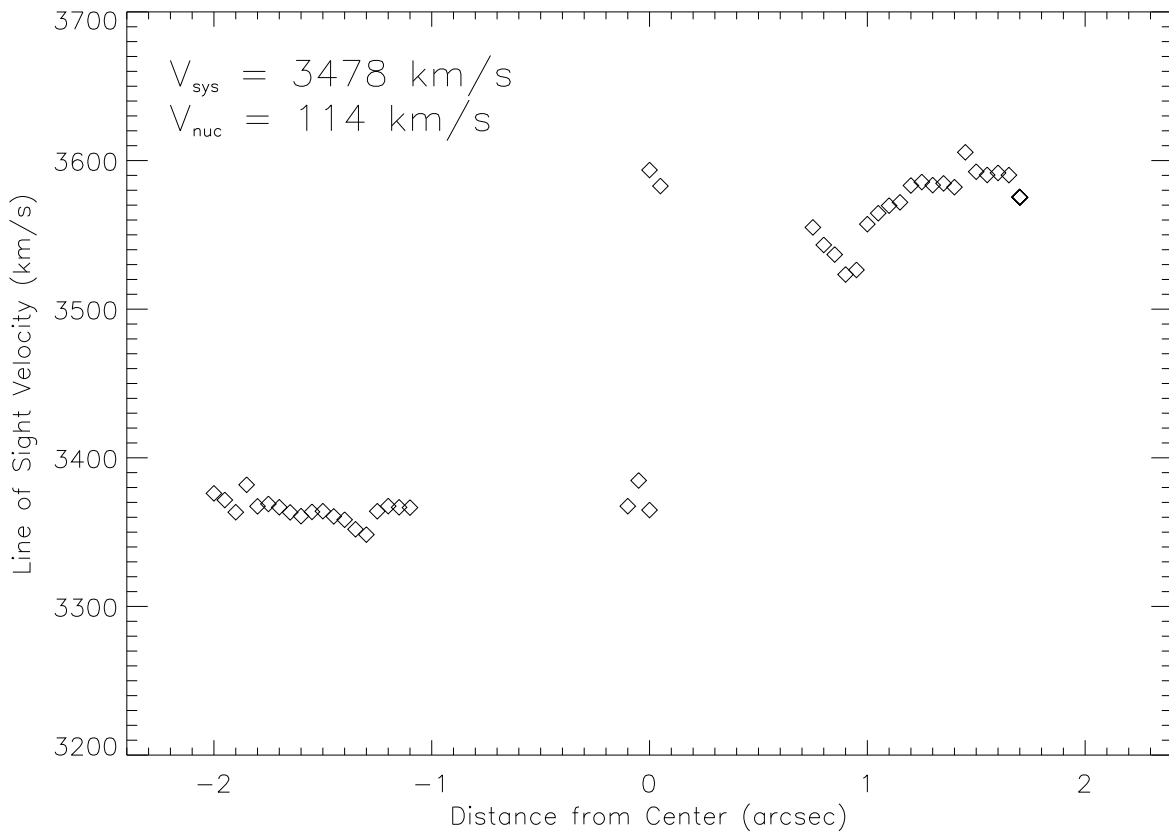


Fig. 5.— H α rotation curve of NGC 5905 measured from 0. $''$ 05 (1 pixel) wide rows on the STIS CCD.

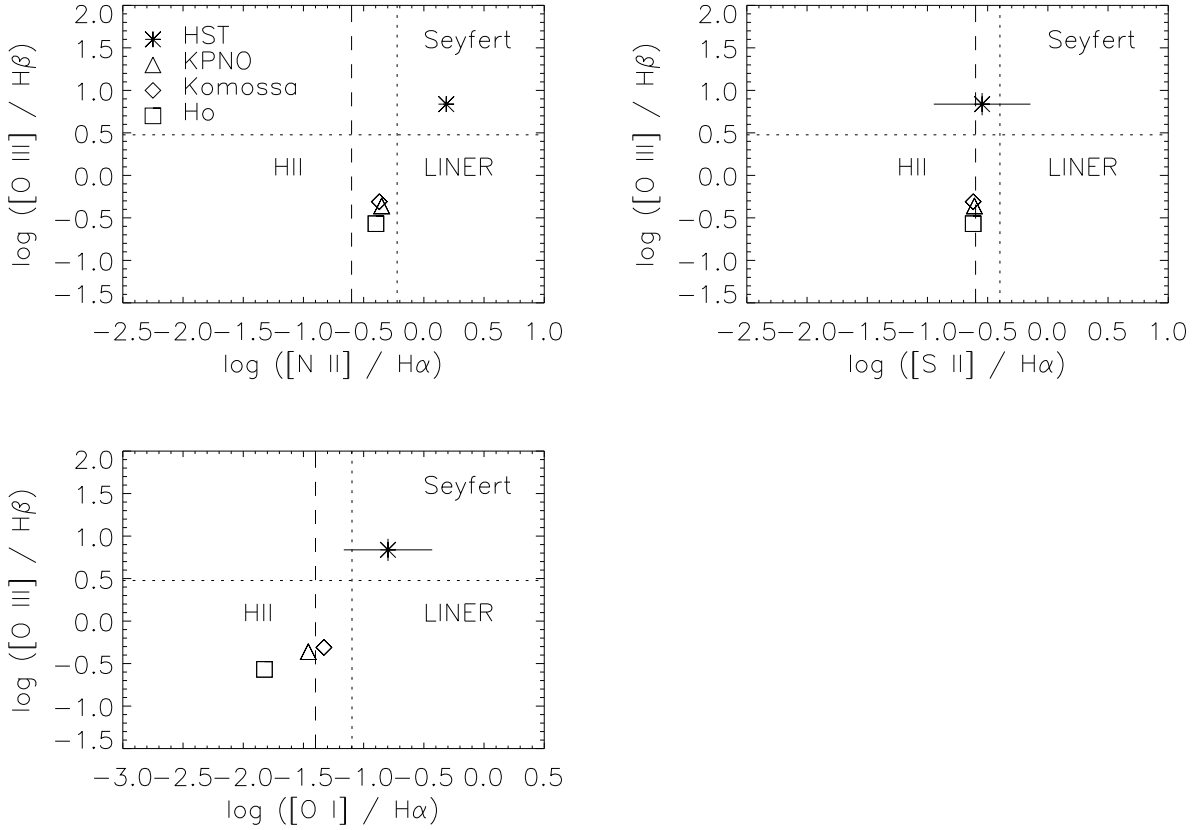


Fig. 6.— Diagnostic diagrams of Veilleux & Osterbrock (1987), with *HST* and various ground-based measurements of emission lines in NGC 5905. The *HST* points are shown with 3σ error bars. The *short dashed* lines are the boundaries separating different classes of objects from Veilleux & Osterbrock (1987), while the *long dashed* line is the classification boundary from Ho et al. (1997).

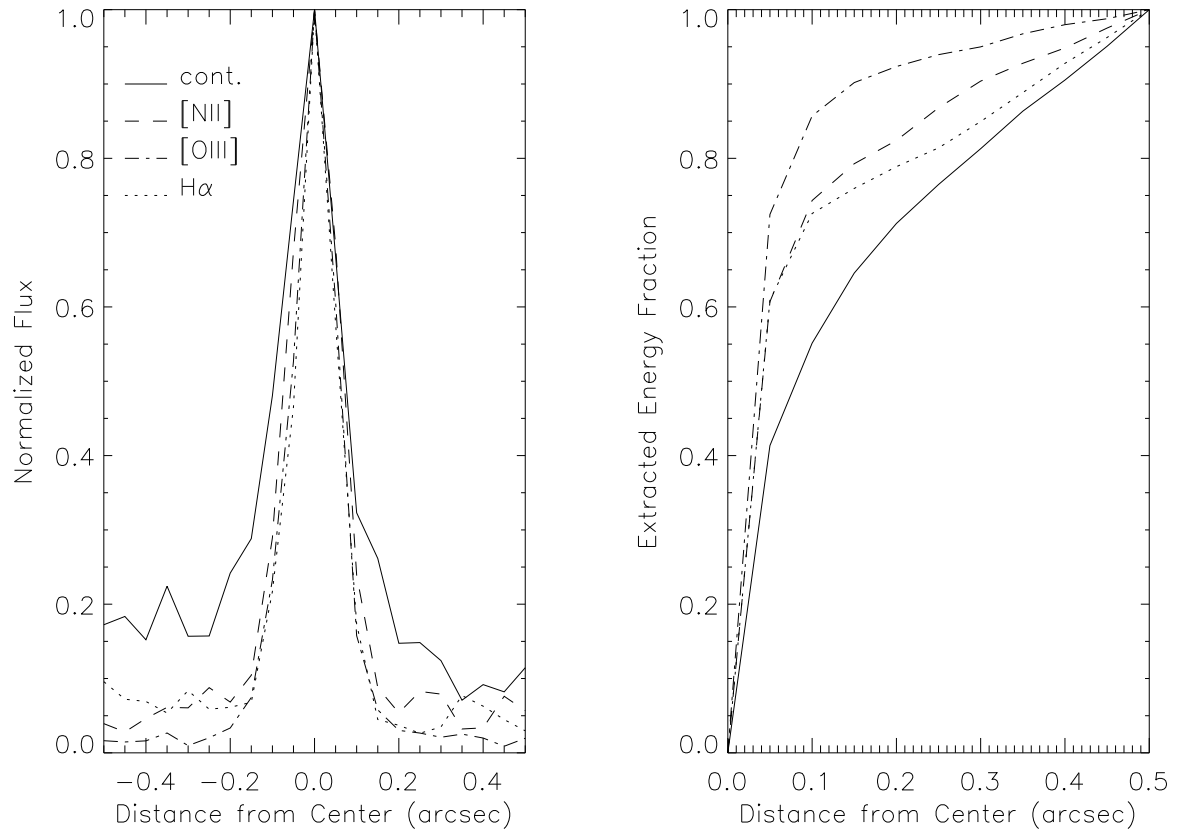


Fig. 7.— Spatial profile of the 2D spectrum of NGC 5905 for [O III], [N II], and H α emission lines perpendicular to the dispersion direction, as well as the profile of the mean continuum from 5480 – 5530 \AA , showing that the starlight is more extended than the nuclear emission lines.

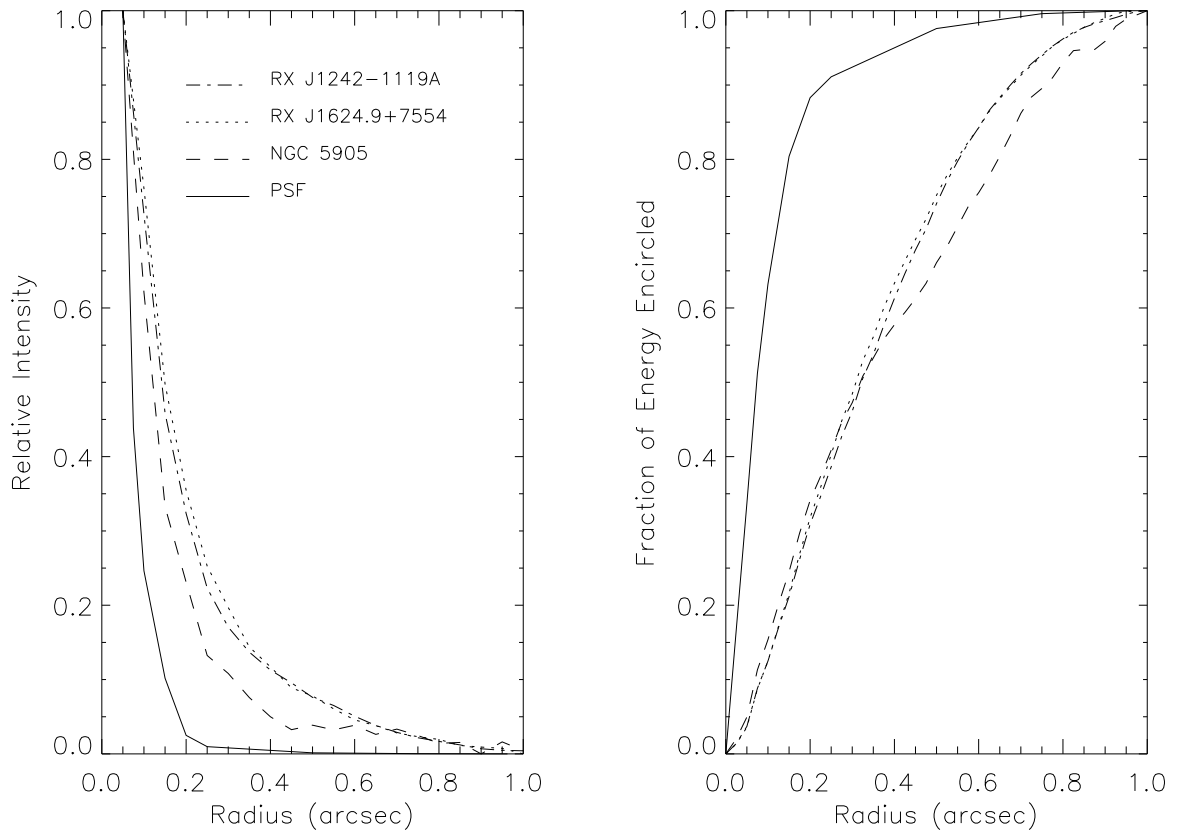


Fig. 8.— Radial profiles of the acquisition image of the three targets, with a background level measured outside of $1''$ subtracted, in comparison with the PSF.